

LSE Precoders for Massive MIMO with Hardware Constraints: Fundamental Limits

M. A. Sedaghat, A. Bereyhi and R. R. Müller, *Senior Member, IEEE*

Abstract

We analyze a general class of nonlinear precoders called Least Square Error (LSE) precoders in multiuser multiple-input multiple-output broadcast channels using the replica method from statistical physics. In LSE precoders, signal on each antenna at base station is limited to be in a predefined set. This predefined set is used to model several hardware constraints such a peak power, constant envelope, discrete constellation constraints. Both Replica Symmetry (RS) and one step Replica Symmetry Breaking (1-RSB) assumptions are applied. For the cases of peak power constrained and constant envelope signals on the transmit antennas, it is shown that the RS assumption provides a good prediction. It is shown that the LSE precoder designed for Peak to Average Power Ratio (PAPR) of 3dB performs as well as the known Regularized Zero Forcing (RZF) precoder with high PAPRs. Moreover, it is shown that constant envelope LSE precoders achieve the same performance as the RZF precoder with about 20% more number of transmit antennas. For PSK signals, the RS assumption gives an optimistic prediction as the inverse load factor, defined as the number of transmit antennas divided by the number of users, increases. Thus, the 1-RSB assumption is applied which gives a better prediction than the RS assumption.

I. INTRODUCTION

In massive Multiple-Input Multiple-Output (MIMO) systems, base stations use a precoder in each coherence interval of the downlink channel to serve multiple users simultaneously [2]. Precoders can be designed to minimize the inter-user interference and consequently the user terminals do not need complicated detection algorithms anymore. This shifts a lot of processing

Mohammad A. Sedaghat, Ali Bereyhi and Ralf R. Müller are with Friedrich-Alexander Universität Erlangen-Nürnberg (e-mails: mohammad.sedaghat@fau.de, ali.bereyhi@fau.de, ralf.r.mueller@fau.de).

A part of this paper has been submitted to IEEE International Conference on Communications (ICC) [1].

from user terminals to base stations which is very attractive for user terminals with limited power.

Several precoding schemes have been proposed so far including linear and nonlinear schemes. Linear schemes mainly consist of Match Filtering (MF), Zero Forcing (ZF) and Regularized Zero Forcing (RZF), where in practice each of them could be preferred regarding the desired tradeoff between the complexity and performance [2], [3]. As examples of nonlinear schemes, one names Tomlinson-Harashima [4] and vector precoding [5]. Precoding design has been also investigated in cases that data constellations of users are finite, e.g., Phase Shift Keying (PSK) constellation [6].

Most of the precoders which have been introduced so far are based on the assumption that base stations can freely transmit any precoded signal without any limitation. This means that signal on each antenna can be chosen from the whole complex plane support. The limitations are on average power or complexity in most of the precoders [7]. However, precoded signals should be transmitted using RF chains and antennas which have some limitations. As an example, to increase the total power efficiency of base stations, nonlinear power amplifiers with low back-off are desired. For low back-off amplifiers, in order to avoid distortion in signals, low Peak-to-Average Power Ratio (PAPR) signals should be used. Thus, precoders with low PAPR output signals are attractive in this case. Furthermore, in recent proposals for MIMO transmitters such as Load Modulated Single-RF (LMSRF) MIMO transmitter, the signal on each antenna cannot be selected freely and possible constellation points on each antenna come from a predefined limited set [8], [9]. In LMSRF transmitters, the number of switches in each load modulator determines the number of possible constellation points. As an example, if every load modulator has only two switches, then each antenna can only transmit signals from a set with cardinality of four. Note that this is different than precoders for finite alphabet signals in which users data symbols are in a finite set but precoded signal can be chosen freely. As an another example, the precoding methods suggested in [10] and [11] are nonlinear precoders designed to keep the envelope of the signal on each antenna constant. Furthermore, in [12], a new nonlinear precoder has been proposed to limit the total instantaneous power. These precoders are among the precoders which are designed using some instantaneous limitations over the precoded signal. In general, one can consider a class of precoders which are designed using the assumption that the signal on each antenna is in a set \mathbb{X} . These types of precoders have not been well studied so far to the best of

our knowledge.

In this paper, we analyze a general class of nonlinear precoders considering the assumption that the signal one each antenna is limited to be in a general set \mathbb{X} . To this end, we select the performance measure of asymptotic distortion at the receiver due to its mathematical tractability. We name these types of precoders as Least Square Error (LSE) precoders which are designed to minimize the asymptotic distortion at the user terminals when the signals on transmit antennas are in a predefined set.

The replica method from statistical physics is used to analyze LSE precoders for a general set \mathbb{X} . We use the Replica Symmetry (RS) assumption together with one step Replica Symmetry Breaking (1-RSB) analysis. A lower bound is also derived for the case of PSK signals. Some special LSE precoders are discussed in details and numerically evaluated.

The rest of this paper is organized as follows: Section II presents the system model for the considered massive MIMO downlink channel and introduces LSE precoders. In Section III, the main theorems of the paper are presented. Some special cases of LSE precoders are analyzed explicitly in Section IV using the RS assumption. In Section V, the rate maximization for LSE precoders is explained. Section VI presents the numerical results and finally the paper is concluded in Section VII.

We use bold lowercase letters for vectors and bold uppercase letters for matrices. Conjugate transpose of a matrix is denoted by \cdot^\dagger , the transpose itself is shown by \cdot^T . Moreover, the real and complex sets are shown by \mathbb{R} and \mathbb{C} , respectively. $F_b(\cdot)$ denotes the cumulative distribution function (cdf) of b and the Kronecker product is shown by \otimes . The real and imaginary parts are denoted by \Re and \Im , respectively, and \mathbb{E} represents the mathematical expectation. Furthermore, we define $Dz \triangleq \frac{1}{\pi}e^{-|z|^2}dz$ and $\text{Vec}(\mathbf{A})$ to be the vector obtained by stacking the columns of \mathbf{A} .

II. SYSTEM MODEL AND PROBLEM FORMULATION

The general problem of designing precoder for a single-cell massive MIMO system with K single-antenna users is considered. The base station is equipped with N antennas. The channel is assumed to be a frequency-flat fading channel. The generalization to the case of frequency-selective fading channels and Orthogonal Frequency Division Multiplexing (OFDM) signals is presented in Appendix E where we show that the same result holds for frequency-selective channels. It is assumed that the channel matrix is perfectly known at the base station and is

used to precode the users data at each coherence interval. Let $\mathbf{u} \in \mathbb{C}^K$ and $\mathbf{H} \in \mathbb{C}^{K \times N}$ be the data vector of the users and the channel matrix, respectively, and $\mathbf{v} \in \mathbb{X}^N$ denotes the precoded vector signal where \mathbb{X} is a predefined set. The received vector at the user terminals reads

$$\mathbf{y} = \mathbf{H}\mathbf{v} + \mathbf{n}, \quad (1)$$

where $\mathbf{y} = [y_1, \dots, y_K]^T$ with y_i being the received signal at the i th user terminal, and \mathbf{n} being the zero mean additive white Gaussian noise vector whose elements have the variance of σ_n^2 . We define the nonlinear LSE precoder with the following rule

$$\mathbf{v} = \underset{\mathbf{x} \in \mathbb{X}^N}{\operatorname{argmin}} \|\mathbf{H}\mathbf{x} - \sqrt{\gamma}\mathbf{u}\|^2 + \lambda\|\mathbf{x}\|^2, \quad (2)$$

where γ is a positive constant and λ is a tuning parameter (Lagrange multiplier) controlling the total transmit power. In case of $\mathbb{X} = \mathbb{C}$, our nonlinear LSE precoding scheme reduces to the linear scheme

$$\mathbf{v} = \sqrt{\gamma}\mathbf{H}^\dagger (\mathbf{H}\mathbf{H}^\dagger + \lambda\mathbf{I})^{-1} \mathbf{u}, \quad (3)$$

which is known as the RZF precoder [3]. The precoding rule, however, does not take a simple form for a general \mathbb{X} . In this paper, we use \mathbb{X} to model different possible hardware constraints in MIMO transmitters. As the first example, one can model peak power constraints on power amplifiers using the set \mathbb{X} as will be explained later. Another example is LMSRF MIMO transmitters in which a finite discrete constellation can be realized due to a finite number of discrete load modulators' states [8], [13]. Another example is the case of constant envelope precoding on each antenna [11] where

$$|v_i|^2 = P \quad \forall i \in \{1, \dots, N\}. \quad (4)$$

In this case, the PAPR is small, around 3 or 4 decibels depending on the pulse shaping filter, and thus highly efficient nonlinear power amplifiers can be utilized. The LSE precoder is able to consider the above hardware constraints and design the precoded signal smartly such that the hardware constraints are fulfilled. In these cases, the classical tools fail to analyze the optimization problem in (2). We therefore invoke the replica method developed in statistical mechanics to determine the large system limit performance of the precoder by calculating the asymptotic distortion defined as

$$D = \lim_{K \uparrow \infty} \frac{1}{K} \mathbb{E} \|\mathbf{H}\mathbf{v} - \sqrt{\gamma}\mathbf{u}\|^2 \quad (5)$$

when the inverse load factor defined as $\alpha \triangleq N/K$, is kept fixed. In fact, the replica method allows us evaluate the asymptotic distortion defined in (5) without finding the explicit solution of the optimization problem (2). Although the exact precoded vector cannot be found through our analysis, it is important in practice to have an estimate of the best performance in order to have a reference performance measure for comparing the practical algorithms.

Throughout the analysis, we set the data symbols of the users to be independent and identically distributed (iid) Gaussian, i.e., $\mathbf{u} \sim \mathcal{CN}(\mathbf{0}, \sigma_u^2 \mathbf{I})$.

The asymptotic distortion measure D can be used to derive a lower bound for the ergodic achievable rate of the users in the downlink channel as follows. Let R_i be the ergodic achievable rate of the i th user. A lower bound for the ergodic rate R_i is obtained when we impose the worst case scenario for the interference at each user terminal which assumes the Gaussian distributed interference at each user terminal. Note that this is true only in the case of Gaussian distributed input signals. Then, we obtain the following bound on the average ergodic rate of the users

$$\frac{1}{K} \sum_{i=1}^K R_i \geq \frac{1}{K} \sum_{i=1}^K \mathbb{E}_{\mathbf{H}} \log \left(1 + \frac{\gamma \sigma_u^2}{\sigma_n^2 + I_i(\mathbf{H})} \right), \quad (6)$$

where $I_i(\mathbf{H})$ is the interference power at the i th user terminal. Using the Jenson's inequality and the fact that the function $\log \left(1 + \frac{\gamma \sigma_u^2}{\sigma_n^2 + x} \right)$ is convex, we obtain

$$\frac{1}{K} \sum_{i=1}^K R_i \geq \log \left(1 + \frac{\gamma \sigma_u^2}{\sigma_n^2 + \frac{1}{K} \sum_{i=1}^K \mathbb{E}_{\mathbf{H}} I_i(\mathbf{H})} \right). \quad (7)$$

It is easy to show that $\frac{1}{K} \sum_{i=1}^K \mathbb{E}_{\mathbf{H}} I_i(\mathbf{H}) = D$ and therefore,

$$\frac{1}{K} \sum_{i=1}^K R_i \geq \log \left(1 + \frac{\gamma \sigma_u^2}{\sigma_n^2 + D} \right). \quad (8)$$

In the case that users have symmetry, e.g., when the users are uniformly distributed in an area, it is easy to show that the ergodic rate of each user is also larger than $\log \left(1 + \frac{\gamma \sigma_u^2}{\sigma_n^2 + D} \right)$.

In this paper we use the replica method to analyze the considered downlink channel with LSE precoder for a general set \mathbb{X} and a general channel matrix \mathbf{H} . The replica method also known as the “replica trick” is a non-rigorous method developed for asymptotic analysis in statistical mechanics. The method has been rigorously justified in some few cases, e.g., for the system whose matrix has a semicircular eigenvalue distribution. Furthermore, it has been shown that

the replica method gives valid predictions for several known problems, and thus it is widely employed for large system analysis of communication systems [14]–[16].

III. LARGE SYSTEM ANALYSIS OF THE LSE PRECODER

In this section, we use the replica method to approximate the asymptotic distortion in the large system limit for a general set \mathbb{X} . Define $\mathbf{R} \triangleq \mathbf{H}^\dagger \mathbf{H}$. We start our analysis by determining

$$\check{D} \triangleq \lim_{K \uparrow \infty} \frac{1}{K} \mathbb{E} \min_{\mathbf{x} \in \mathbb{X}^N} \|\mathbf{H}\mathbf{x} - \sqrt{\gamma}\mathbf{u}\|^2 + \lambda \|\mathbf{x}\|^2 \quad (9)$$

which reads

$$\check{D} = \gamma\sigma_u^2 + \lim_{K \uparrow \infty} \frac{1}{K} \mathbb{E} \min_{\mathbf{x} \in \mathbb{X}^N} g(\mathbf{x}) \quad (10)$$

with the function $g(\mathbf{x})$ being defined as

$$g(\mathbf{x}) \triangleq \mathbf{x}^\dagger \mathbf{R} \mathbf{x} - 2\sqrt{\gamma} \Re \{ \mathbf{x}^\dagger \mathbf{H}^\dagger \mathbf{u} \} + \lambda \mathbf{x}^\dagger \mathbf{x}. \quad (11)$$

Using Varadhan's theorem [17], the minimization in (10) can be converted to

$$\min_{\mathbf{x} \in \mathbb{X}^N} g(\mathbf{x}) = - \lim_{\beta \uparrow \infty} \frac{1}{\beta} \log \sum_{\mathbf{x} \in \mathbb{X}^N} e^{-\beta g(\mathbf{x})}. \quad (12)$$

The parameter β is called the inverse temperature in the equivalent thermodynamic system [18]. It is observed from (10) and (12) that the evaluation of \check{D} needs a logarithmic expectation to be determined which is not a trivial task for a general set \mathbb{X} . Thus, we use the equality

$$\mathbb{E} \log(t) = \lim_{n \downarrow 0} \frac{\partial}{\partial n} \log \mathbb{E} t^n, \quad (13)$$

for some positive random variable t . Consequently, we have

$$\check{D} = \gamma\sigma_u^2 - \lim_{K, \beta \uparrow \infty} \frac{1}{\beta K} \lim_{n \downarrow 0} \frac{\partial}{\partial n} \log \mathbb{E} \left[\sum_{\mathbf{x} \in \mathbb{X}^N} e^{-\beta g(\mathbf{x})} \right]^n \triangleq \gamma\sigma_u^2 - \lim_{\beta \uparrow \infty} \frac{1}{\beta} \lim_{n \downarrow 0} \frac{\partial}{\partial n} \Xi_n, \quad (14)$$

where Ξ_n denotes the corresponding term in (14). Here, the replica method suggests us to consider the replica continuity assumption and do the further analysis as follows: First, determine Ξ_n for an integer n , and then, assume that the analytic continuation of Ξ_n onto the real line gives the same result in the neighborhood of $n = 0$. For details about the validity of this assumption, the reader is referred to [18]. When n is integer, we have

$$\Xi_n = \lim_{K \uparrow \infty} \frac{1}{K} \log \mathbb{E} \left[\sum_{\mathbf{x} \in \mathbb{X}^N} e^{-\beta g(\mathbf{x})} \right]^n = \lim_{K \uparrow \infty} \frac{1}{K} \log \sum_{\{\mathbf{x}_a\}} \mathbb{E} e^{-\beta \sum_{a=1}^n g(\mathbf{x}_a)} \quad (15)$$

where $\{\mathbf{x}_a\}$ denotes the replicas $\{\mathbf{x}_1, \dots, \mathbf{x}_n\} \in \mathbb{X}^N \times \dots \times \mathbb{X}^N$. Using the independency of \mathbf{u} and \mathbf{H} , the expectations over \mathbf{u} and \mathbf{H} separate. Thus, by taking the expectation over \mathbf{u} with Gaussian iid entries, the summation on the right hand side of (15) reduces to

$$\sum_{\{\mathbf{x}_a\}} \mathbb{E} e^{-\beta \sum_{a=1}^n \mathbf{g}(\mathbf{x}_a)} = \sum_{\{\mathbf{x}_a\}} \mathbb{E}_{\mathbf{H}} e^{-\beta \sum_{a=1}^n [\mathbf{x}_a^\dagger \mathbf{R} \mathbf{x}_a + \lambda \mathbf{x}_a^\dagger \mathbf{x}_a] + \beta^2 \gamma \sigma_u^2 \|\sum_{a=1}^n \mathbf{H} \mathbf{x}_a\|^2}, \quad (16)$$

where $\mathbb{E}_{\mathbf{H}}$ denotes the expectation with respect to \mathbf{H} . By defining the matrix \mathbf{V} as

$$\mathbf{V} \triangleq \frac{1}{N} [\mathbf{x}_1, \dots, \mathbf{x}_n] \Gamma [\mathbf{x}_1, \dots, \mathbf{x}_n]^\dagger \quad (17)$$

with Γ being an $n \times n$ matrix with entries

$$\zeta_{i,j} \triangleq -\beta \gamma \sigma_u^2 + \delta_{i,j}, \quad (18)$$

Ξ_n is found as

$$\Xi_n = \lim_{K \uparrow \infty} \frac{1}{K} \log \sum_{\{\mathbf{x}_a\}} e^{-\beta \lambda \sum_{a=1}^n \mathbf{x}_a^\dagger \mathbf{x}_a} \mathbb{E}_{\mathbf{H}} e^{-\beta N \text{tr}(\mathbf{R} \mathbf{V})}. \quad (19)$$

Suppose that the empirical distribution of the eigenvalues of \mathbf{R} converges to a deterministic distribution, and denote the corresponding cdf with $F_{\mathbf{R}}(\lambda)$. The Stieltjes transform of the distribution $F_{\mathbf{R}}(\lambda)$ is defined as $G_{\mathbf{R}}(s) = \mathbb{E}(\lambda - s)^{-1}$. The corresponding R-transform is then defined as

$$R_{\mathbf{R}}(w) = G_{\mathbf{R}}^{-1}(w) - w^{-1} \quad (20)$$

where $G_{\mathbf{R}}^{-1}(w)$ denotes the inverse with respect to composition. Noting that the expectation in (19) is a spherical integral, we use the results from [19] which state

$$\mathbb{E}_{\mathbf{H}} e^{-\beta N \text{tr}(\mathbf{R} \mathbf{V})} = e^{-N \sum_{i=1}^N \int_0^{\beta \tilde{\lambda}_i} R_{\mathbf{R}}(-w) dw}, \quad (21)$$

as $N \uparrow \infty$ with $\tilde{\lambda}_1, \dots, \tilde{\lambda}_N$ being the eigenvalues of \mathbf{V} . The matrix \mathbf{V} has only n nonzero eigenvalues which are equal to the eigenvalues of ¹

$$\mathbf{G} = \frac{1}{N} \Gamma [\mathbf{x}_1, \dots, \mathbf{x}_n]^\dagger [\mathbf{x}_1, \dots, \mathbf{x}_n]. \quad (22)$$

Consequently, denoting the eigenvalues of \mathbf{G} by $\lambda_1, \dots, \lambda_n$, we have

$$\mathbb{E}_{\mathbf{H}} e^{-\beta N \text{tr}(\mathbf{R} \mathbf{V})} = e^{-N \left(\sum_{i=1}^n \int_0^{\beta \lambda_i} R_{\mathbf{R}}(-w) dw + \epsilon_N \right)}, \quad (23)$$

¹This can be easily shown using the fact that the nonzero eigenvalues of the two matrices \mathbf{AB} and \mathbf{BA} are the same.

where ϵ_N tends to zero when $N \uparrow \infty$. From (19), it is observed that in order to find Ξ_n , it is required to sum over the Nn -dimensional space. Here we utilize the same approach as in [15] by splitting the space into the subshells

$$\mathcal{S}(\mathbf{Q}) \triangleq \{\mathbf{x}_1, \dots, \mathbf{x}_n | \mathbf{x}_a^\dagger \mathbf{x}_b = N Q_{ab}\}, \quad (24)$$

where Q_{ab} is the (a, b) th entry of the matrix

$$\mathbf{Q} = \frac{1}{N} [\mathbf{x}_1, \dots, \mathbf{x}_n]^\dagger [\mathbf{x}_1, \dots, \mathbf{x}_n]. \quad (25)$$

In each subshell, the inner product of two replicated vectors \mathbf{x}_a and \mathbf{x}_b is constant [15]. Then, in (19), Ξ_n is calculated as

$$\Xi_n = \lim_{K \uparrow \infty} \frac{1}{K} \log \int e^{N\mathcal{I}(\mathbf{Q})} e^{-N\mathcal{G}(\mathbf{Q})} \mathcal{D}\mathbf{Q}, \quad (26)$$

where the function $\mathcal{G}(\mathbf{Q})$ is defined as

$$\mathcal{G}(\mathbf{Q}) \triangleq \beta \lambda \sum_{a=1}^n \frac{\mathbf{x}_a^\dagger \mathbf{x}_a}{N} + \sum_{i=1}^n \int_0^{\beta \lambda_i} R_{\mathbf{R}}(-w) dw, \quad (27)$$

and $e^{N\mathcal{I}(\mathbf{Q})}$ is the Jacobian of the integral; moreover, we define

$$\mathcal{D}\mathbf{Q} \triangleq \prod_{a=1}^n \prod_{b=a+1}^n d\Re Q_{ab} d\Im Q_{ab}. \quad (28)$$

The Jacobian term in (26) is calculated as

$$e^{N\mathcal{I}(\mathbf{Q})} = \int \prod_{a \leq b} \delta(\Re [\mathbf{x}_a^\dagger \mathbf{x}_b - N Q_{ab}]) \delta(\Im [\mathbf{x}_a^\dagger \mathbf{x}_b - N Q_{ab}]) \prod_{a=1}^n dF_{\mathbf{x}}(\mathbf{x}_a). \quad (29)$$

Then, we introduce a new matrix $\tilde{\mathbf{Q}}$ in the complex frequency domain. Following the lines in [15, eq.(52)-(58)] and defining $\mathcal{J} \triangleq (t - j\infty; t + j\infty)$ for some $t \in \mathbb{R}$, we obtain

$$e^{N\mathcal{I}(\mathbf{Q})} = \int_{\mathcal{J}^{n^2}} e^{-N \text{tr}[\tilde{\mathbf{Q}} \mathbf{Q}] + N \log \mathcal{M}(\tilde{\mathbf{Q}})} \tilde{\mathcal{D}}\tilde{\mathbf{Q}} \quad (30)$$

where the function $\mathcal{M}(\tilde{\mathbf{Q}})$ is defined as

$$\mathcal{M}(\tilde{\mathbf{Q}}) \triangleq \sum_{\{\mathbf{x}_a\}} e^{\sum_{a,b} x_a^* x_b \tilde{Q}_{ab}}, \quad (31)$$

and $\tilde{\mathcal{D}}\tilde{\mathbf{Q}}$ is given in [15, eq.(57)]. In the large system limit, the integration in (26) is dominated by the integrand at the saddle point. In order to calculate the saddle point of the integrand, one

needs to impose a structure on the matrices \mathbf{Q} and $\tilde{\mathbf{Q}}$. The most primary structure is imposed by the RS assumption. In the RS assumption, it is postulated that the saddle point matrices which dominate the integration in (26) are invariant to permutation of the replica indices. Therefore, following [15], under the RS assumption we set $Q_{a,b} = q$ and $\tilde{Q}_{a,b} = \beta^2 f^2$ for all $a \neq b$ and $Q_{a,a} = q + \chi/\beta$ and $\tilde{Q}_{a,a} = \beta^2 f^2 - \beta e$ for all a where $\{q, \chi, f, e\}$ are some positive finite constants. Substituting the RS structure in (26), Ξ_n can be analytically calculated, and consequently, \tilde{D} is determined accordingly. The final expression for the asymptotic distortion under the RS assumption is stated in Proposition 1.

PROPOSITION 1 Under the RS assumption, the asymptotic distortion converges to

$$D = \gamma \sigma_u^2 + \alpha \frac{\partial}{\partial \chi} \left[(q - \chi \gamma \sigma_u^2) \chi R_{\mathbf{R}}(-\chi) \right], \quad (32)$$

as $K, N \uparrow \infty$ and the inverse load factor α is kept fixed. q and χ are solutions to the following two coupled equations

$$\chi = \frac{1}{f} \Re \int_{\mathbb{C}} \operatorname{argmin}_{x \in \mathbb{X}} \left| z - \frac{R_{\mathbf{R}}(-\chi) + \lambda}{f} x \right| z^* Dz \quad (33)$$

$$q = \int_{\mathbb{C}} \left| \operatorname{argmin}_{x \in \mathbb{X}} \left| z - \frac{R_{\mathbf{R}}(-\chi) + \lambda}{f} x \right| \right|^2 Dz \quad (34)$$

where

$$f \triangleq \sqrt{(q - \chi \gamma \sigma_u^2) R'_{\mathbf{R}}(-\chi) + \gamma \sigma_u^2 R_{\mathbf{R}}(-\chi)}. \quad (35)$$

■

The proof of Proposition 1 is given in Appendix A.

Although the RS assumption has been shown to give the exact solution for some problems [20]–[22], there are several examples (mostly non-convex and combinatorics problems) in which this assumption fails to give a valid prediction [16]. For these cases, in order to have a more precise prediction, one needs to employ the r -step RSB assumption which imposes a more generalized structure on the matrices \mathbf{Q} and $\tilde{\mathbf{Q}}$. Here, we consider the 1-RSB assumption which postulates [16]

$$\mathbf{Q} = q_1 \mathbf{1}_n + p_1 \mathbf{I}_{\frac{n\beta}{\mu_1}} \otimes \mathbf{1}_{\frac{\mu_1}{\beta}} + \frac{\chi_1}{\beta} \mathbf{I}_n, \quad (36)$$

$$\tilde{\mathbf{Q}} = \beta^2 f_1^2 \mathbf{1}_n + \beta^2 g_1^2 \mathbf{I}_{\frac{n\beta}{\mu_1}} \otimes \mathbf{1}_{\frac{\mu_1}{\beta}} - \beta e_1 \mathbf{I}_n, \quad (37)$$

where $q_1, p_1, \chi_1, \mu_1, f_1, g_1, e_1$ are non-negative real numbers, $\mathbf{1}_n$ is an $n \times n$ all-ones matrix and \mathbf{I}_n is the $n \times n$ identity matrix. Note that for more than one step breaking assumptions, the calculation becomes too complicated, though basically possible. Employing the 1-RSB structure, Proposition 2 shows the estimated asymptotic distortion.

PROPOSITION 2 Under the 1-RSB assumption, the asymptotic distortion converges to

$$D = \gamma\sigma_u^2 - \frac{\alpha\chi_1}{\mu_1}R_{\mathbf{R}}(-\chi_1) + \alpha \left[q_1 + \frac{\eta_1}{\mu_1} - 2\gamma\sigma_u^2\eta_1 \right] R_{\mathbf{R}}(-\eta_1) - \alpha\eta_1 [q_1 - \gamma\sigma_u^2\eta_1] R'_{\mathbf{R}}(-\eta_1), \quad (38)$$

as $K, N \uparrow \infty$ and the inverse load factor α is kept fixed. The set of scalars $\{q_1, p_1, \chi_1, \mu_1\}$ is calculated through the coupled equations

$$\begin{aligned} \eta_1 &= \frac{1}{f_1} \int \int \Re \{ z^* \operatorname{argmin} |f_1 z + g_1 y - e_1 x| \} \tilde{\mathcal{Y}}(y, z) Dz Dy, \\ q_1 + p_1 &= \int \int |\operatorname{argmin} |f_1 z + g_1 y - e_1 x||^2 \tilde{\mathcal{Y}}(y, z) Dz Dy, \\ \eta_1 + \mu_1 q_1 &= \frac{1}{g_1} \int \int \Re \{ y^* \operatorname{argmin} |f_1 z + g_1 y - e_1 x| \} \tilde{\mathcal{Y}}(y, z) Dz Dy, \end{aligned} \quad (39)$$

and

$$\begin{aligned} \int_{\chi_1}^{\eta_1} R_{\mathbf{R}}(-w) dw &= \int \log \int \mathcal{Y}(y, z) Dy Dz - 2\chi_1 R_{\mathbf{R}}(-\chi_1) \\ &\quad + (\mu_1 q_1 + 2\eta_1 - 2\mu_1 \eta_1 \gamma \sigma_u^2 - 2\chi_1 \mu_1 \gamma \sigma_u^2) R_{\mathbf{R}}(-\eta_1) \\ &\quad - 2\mu_1 \eta_1 (q_1 - \gamma \sigma_u^2 \eta_1) R'_{\mathbf{R}}(-\eta_1) + \lambda \mu_1 (p_1 + q_1), \end{aligned} \quad (40)$$

where $\eta_1 = \chi_1 + \mu_1 p_1$,

$$\mathcal{Y}(y, z) = e^{-\mu_1 \min_{x \in \mathbb{X}} e_1 |x|^2 - 2\Re \{ x(f_1 z^* + g_1 y^*) \}}, \quad (41)$$

and the function $\tilde{\mathcal{Y}}(y, z)$ being defined as

$$\tilde{\mathcal{Y}}(y, z) = \frac{\mathcal{Y}(y, z)}{\int_{\mathbb{C}} \mathcal{Y}(\tilde{y}, z) D\tilde{y}}. \quad (42)$$

Moreover, the parameters $\{e_1, f_1, g_1\}$ are determined as

$$\begin{aligned} e_1 &= R_{\mathbf{R}}(-\chi_1) + \lambda \\ f_1 &= \sqrt{\gamma \sigma_u^2 R_{\mathbf{R}}(-\eta_1) + (q_1 - \gamma \sigma_u^2 \eta_1) R'_{\mathbf{R}}(-\eta_1)} \\ g_1 &= \sqrt{\frac{R_{\mathbf{R}}(-\chi_1) - R_{\mathbf{R}}(-\eta_1)}{\mu_1}}. \end{aligned} \quad (43)$$

■

The proof of Proposition 2 is given in Appendix B.

Note that letting $p_1 = 0$ reduces the 1-RSB solution to the RS solution. This means that one of the 1-RSB solutions is always the RS solution. The coupled equations in both the RS and 1-RSB cases may have multiple solutions, though only one of them is the valid saddle point of (26). In this case, the saddle point is the solution which minimizes a function corresponding to the system, known as the free energy [18]. It can be shown that the free energy of the nonlinear LSE precoder is $-\check{D}$. This means that the actual solution is the solution which maximizes \check{D} . Therefore, to obtain the actual solution of the coupled equations, we always need to check the value of the free energy for all the solutions and decide which solution is the actual one.

In order to validate the prediction of the replica method in statistical physics, one way is to check the entropy of the corresponding thermodynamic system [16]. The entropy values close to 0 show that the solution is reliable. With the same analysis as in [16, Proposition IV.5], one can show that the entropy in the problem of LSE precoding is

$$\mathcal{H}_{\text{RS}} = \zeta R_{\mathbf{R}}(-\zeta) - \int_0^{\zeta} R_{\mathbf{R}}(-w)dw, \quad (44)$$

where $\zeta = \chi$ for the RS solution, and $\zeta = \chi_1$ for the 1-RSB solution.

IV. THE RS SOLUTION FOR SOME SPECIAL CASES

In this section, we derive the RS prediction of the LSE precoder performance considering some hardware constraints in massive MIMO base stations. The 1-RSB solution in these cases can be calculated in a similar way, although the calculations are more complicated. Thus, here due to the lack of space, we only present the RS solutions and the 1-RSB predictions for some cases are also given in the numerical results section.

Although the results in Proposition 1, 2 are for a general channel matrix, here we first consider a $K \times N$ channel matrix whose elements are iid with variance of $\frac{1}{N}$. Note that the results do not depend on the distribution of the entries of the channel matrix and the iid assumption is enough here. The iid channel model holds in reach scattering environments when a perfect power control is employed at user terminals. We later in Appendix D discuss the effect of path loss of the users when there is no power control. For a matrix whose elements are iid with variance of $\frac{1}{N}$,

we have [23]

$$R_{\mathbf{R}}(w) = \frac{\frac{1}{\alpha}}{1-w}. \quad (45)$$

In the following subsections, we derive the result of Proposition 1 explicitly for several cases.

A. Peak power constraint on each antenna and total average power constraint

Let's consider the case in which the instantaneous power on each antenna at the base station is constrained by P and the total average power is also limited. Thus, the set \mathbb{X} is determined by

$$\mathbb{X} = \left\{ x = r e^{j\theta} \mid \theta \in [0, 2\pi], 0 \leq r \leq \sqrt{P} \right\}. \quad (46)$$

The total power normalized by N is shown by q in the replica analysis. Hence, we fix q in the coupled equations and calculate the corresponding λ to reach such an average power. The RS coupled equations in (33) and (34) are simplified to

$$\begin{aligned} \chi &= \sqrt{\frac{\alpha}{q + \gamma\sigma_u^2}}(1 + \chi)h, \\ q &= c^2 \left(1 - e^{-\frac{P}{c^2}} \right), \end{aligned} \quad (47)$$

where

$$h = \int_{|z| \leq \frac{\sqrt{P}}{c}} c|z|^2 \frac{e^{-|z|^2}}{\pi} dz + \int_{|z| > \frac{\sqrt{P}}{c}} \sqrt{P}|z| \frac{e^{-|z|^2}}{\pi} dz = c - ce^{-\frac{P}{c^2}} + \sqrt{P\pi}Q\left(\frac{\sqrt{2P}}{c}\right), \quad (48)$$

and

$$c = \frac{\sqrt{\alpha(q + \gamma\sigma_u^2)}}{\alpha\lambda(1 + \chi) + 1}. \quad (49)$$

Finally, the asymptotic distortion is calculated as

$$D = \lim_{K \uparrow \infty} \frac{1}{K} \mathbb{E} \min_{\mathbf{x} \in \mathbb{X}^N} \|\mathbf{Hx} - \mathbf{u}\|^2 = \frac{q + \gamma\sigma_u^2}{(1 + \chi)^2}. \quad (50)$$

B. M-PSK signals on antennas

In this case, we consider M-PSK signal on each antenna as

$$\mathbb{X} = \left\{ \sqrt{q} e^{j \frac{2\pi}{M}}, \sqrt{q} e^{j \frac{4\pi}{M}}, \sqrt{q} e^{j \frac{6\pi}{M}}, \dots, \sqrt{q} e^{j 2\pi} \right\}. \quad (51)$$

This models the case that the signal on each antenna in the base station can be only chosen from a PSK constellation. This limitation appears in load-modulated single-RF MIMO transmitters in which due to the limited number of states of the load modulators, the signal constellation is limited. Note that in this case, the average power q is imposed by the set \mathbb{X} , thus we only need to determine χ in the coupled equations. Since $\|\mathbf{x}\|^2$ is constant for PSK constellations, the minimization in (2) leads to $\lambda = 0$, although λ has no impact on the result in this case. The coupled equations in Proposition 1 reduce to

$$\chi = \frac{1}{\frac{2}{M \sin(\pi/M)} \sqrt{\pi \frac{q + \gamma \sigma_u^2}{q\alpha}} - 1}, \quad (52)$$

and the asymptotic distortion reads

$$D = \frac{q + \gamma \sigma_u^2}{(1 + \chi)^2}. \quad (53)$$

The case of constant envelope signal is easily obtained by letting $M \rightarrow \infty$. In this case, (52) becomes

$$\chi = \frac{1}{2 \sqrt{\frac{q + \gamma \sigma_u^2}{\pi q \alpha}} - 1}. \quad (54)$$

From (52) and (53), it is observed that there is a finite α^* that for $\alpha \uparrow \alpha^*$, χ goes to infinity and the asymptotic distortion converges to zero. In Appendix C, we derive a lower bound for the asymptotic distortion for M-PSK signals and show that for finite α s, the distortion for M-PSK signals is nonzero. This result shows that the RS prediction is not precise in the case of PSK signals for the load factor close to α^* . Note that if we assume that r -RSB solution when $r \rightarrow \infty$ gives the actual solution, then the solution derived by RS is a lower bound for the actual distortion since the free energy here is equal to minus of the asymptotic distortion. In the numerical results section, we present the 1-RSB prediction for PSK signals which is observed to be a better estimation.

V. OPTIMIZING THE LSE PERFORMANCE

In the LSE precoder, λ is a parameter which controls the average transmit power at the base station and γ is the power gain of the signals of the users at their receivers. Note that γ affects the transmit power as well. In this section, we explain how to design λ and γ to get the best performance. In every communication system, power is limited, hence we fix the average transmit power q . Then, in the replica analyses we have one degree of freedom. As an example, in the RS analysis for a given q , we have the variables χ, γ, λ and two coupled equations. This degree of freedom allows us to maximize the lower bound of the rate for a given set of $q, \sigma_n^2, \sigma_u^2$. Here we take the example of RZF precoder and the numerical results for the other cases will be presented in the results section. In RZF precoder, we have $\mathbb{X} = \mathbb{C}$, thus the coupled equations become

$$q = \frac{\alpha(q + \gamma\sigma_u^2)}{[1 + \lambda\alpha(1 + \chi)]^2}, \quad (55)$$

$$\chi = \frac{\alpha(1 + \chi)}{1 + \lambda\alpha(1 + \chi)}. \quad (56)$$

We consider the variable χ as the free variable due to the simplicity and obtain all the other variables as functions of χ . Thus, we obtain

$$\lambda = \frac{1}{\chi} - \frac{1}{\alpha(1 + \chi)} \quad (57)$$

$$\gamma = \frac{q}{\sigma_u^2} \left[\frac{\alpha(1 + \chi)^2}{\chi^2} - 1 \right] \quad (58)$$

$$D = \frac{q\alpha}{\chi^2}. \quad (59)$$

Furthermore, the lower bound for the normalized sum rate reads

$$\frac{1}{K} \sum_{i=1}^K R_i \geq \log \left(1 + \frac{q}{\sigma_n^2} \frac{\alpha(1 + \chi)^2 - \chi^2}{\chi^2 + \alpha \frac{q}{\sigma_n^2}} \right). \quad (60)$$

We wish to maximize the right-hand-side of (60). Let $s \stackrel{\triangle}{=} \frac{q}{\sigma_n^2}$. It is easy to show that the right-hand-side of (60) has only one local maximum for $\chi \geq 0$. Therefore, by taking derivative from the right-hand-side of (60), we get

$$\chi_{\text{opt}} = \frac{1}{2} \left((\alpha - 1)s - 1 + \sqrt{((\alpha - 1)s - 1)^2 + 4\alpha} \right), \quad (61)$$

and the optimum value for λ is obtained by substituting (61) in (57) as

$$\lambda_{\text{opt}} = \frac{2}{(\alpha - 1)s - 1 + \sqrt{((\alpha - 1)s - 1)^2 + 4\alpha}} - \frac{2}{\alpha((\alpha - 1)s + \sqrt{((\alpha - 1)s - 1)^2 + 4\alpha})}. \quad (62)$$

One can do the same procedure for every given set \mathbb{X} and derive λ_{opt} . We will show some numerical results for per-antenna peak power, constant envelope and PSK cases in the results section.

VI. NUMERICAL RESULTS

In this section, the performance of the LSE precoder for some hardware constraints is investigated. We use the two introduced measures: the asymptotic distortion D and the lower bound for the sum rate $\frac{1}{K} \sum_{k=1}^K R_k$. Furthermore, without loss of generality we set $\sigma_u^2 = 1$.

A. Peak and average power constraints

In this subsection, we consider per-antenna peak and total average power constraints at the base station. The optimization problem (2) in this case is convex. Although, it has not been proven rigorously, it is generally believed in the literature that the RS assumption is valid for convex problems. Thus, we take the RS solution and check the validity of this assumption by means of simulation.

Fig. 1 represents the asymptotic distortion versus the inverse load factor for a fixed total average power $q = 0.5$, different PAPR defined as P/q and $\gamma = 1$. To validate the results by the replica method, we have also plotted some simulation results obtained by the CVX toolbox for $K = 200$. In the simulation, we minimize the asymptotic distortion considering average and per-antenna power constraints imposed by q and P . From Fig. 1, it is observed that the simulation results confirm the RS prediction. For PAPRs equal to or more than 3 dB, the asymptotic distortion is sufficiently close to the case without peak power constraint (which is RZF in this case). The curve for PAPR = 0dB describes the case of constant envelope signals.

In order to describe the variation of the required average power for a fixed asymptotic distortion with respect to the number of transmit antennas, we consider the case with unit per-antenna peak power constraint and plot the average power per-antenna for some given asymptotic distortions. The parameter γ is set to 1. The results are shown in Fig. 2. It is observed that the per-antenna average power decays by increasing α . By numerical curve fitting, it can be observed that the per-antenna average power converges to $c\alpha^\kappa$ for some constants c and $\kappa = -1$ as α grows large. For finite α , however, $\kappa < -1$. For massive MIMO systems, i.e., $\alpha \gg 1$, with average power constraint, it has been shown that when the base station has perfect channel state information,

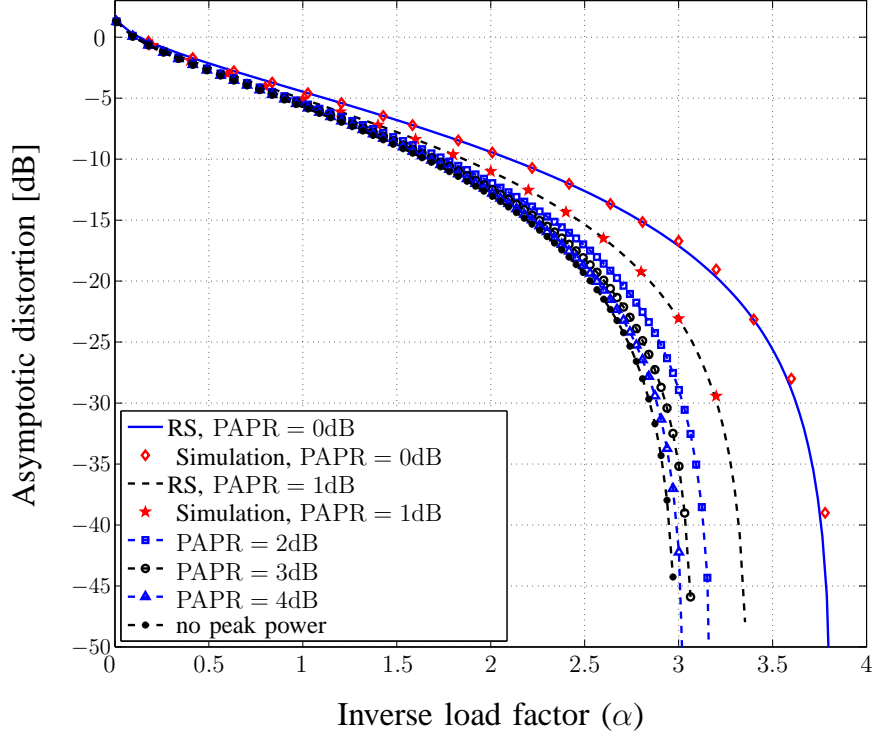


Fig. 1: Asymptotic distortion versus the inverse load factor, i.e., $\alpha = N/K$, for different peak power values on each transmit antenna when the per-antenna average power is set to 0.5.

signal to interference plus noise ratio can be improved by a factor of α , asymptotically [2] which agrees the result given here for the peak power constraint.

Next, the achievable sum rate normalized by the number of users derived in (8) is investigated. The noise variance σ_n^2 and the average transmitted power q are set to 1. The parameters λ and γ are chosen such that the achievable rate is maximized. In Fig. 3, the achievable sum rate normalized by the number of users is plotted versus the inverse load factor for different peak to average power constraints. Note that although the replica method also predicts the results for $\alpha < 1$, the valid system assumption here is $\alpha \geq 1$ since the number of base station antennas should be larger than the number of users. The rate for different PAPRs are quit close. At around $\alpha = 5$, for the case of constant envelope signal we need about 20% more antennas to obtain the same performance as in the case of no peak power constraint.

In Fig. 4, we fix $\alpha = 5$ and change the noise power to investigate the achievable rate versus Signal-to-Noise Ratio (SNR) defined as $\frac{q}{\sigma_n^2}$. Furthermore, we set $q = 1$ and the other parameters

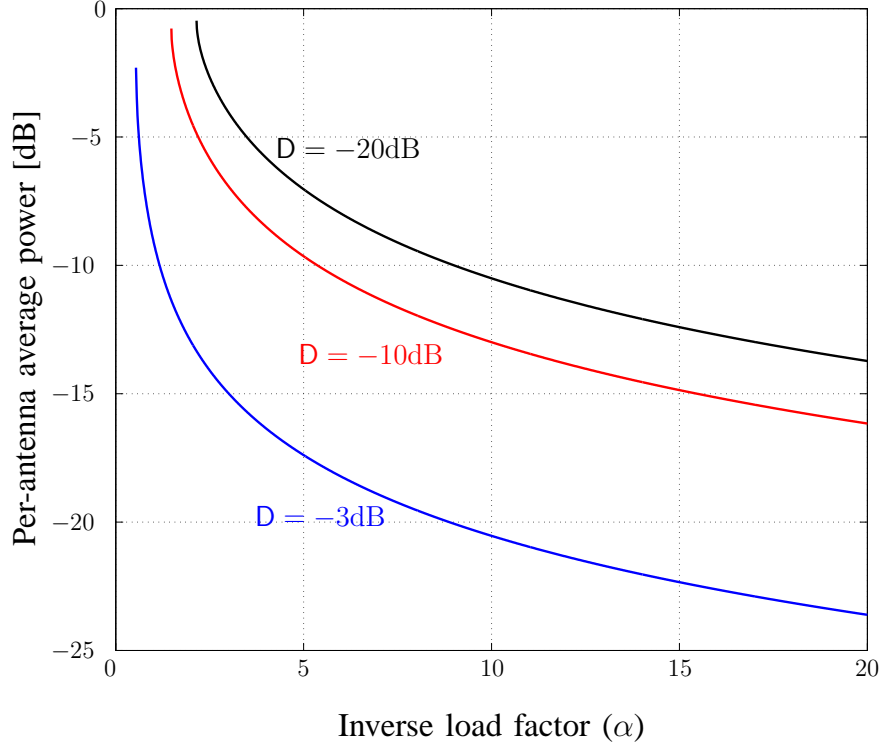


Fig. 2: Required per-antenna average power versus the inverse load factor, i.e., $\alpha = N/K$, for different asymptotic distortions and $P = 1$.

are calculated to optimize the achievable rate. The results show that for $\alpha = 5$, about 1.3dB more transmit power is required to get the same performance compared to the case of no peak power constraint.

B. PSK signals

In this subsection, we investigate the case of PSK signals on each antenna at the base station. The first interesting question here is whether the RS assumption is a valid assumption. Note that for discrete signals like PSK, the optimization problem in (2) is a combinatoric problem. We take BPSK and QPSK and use both RS and 1-RSB solutions. Furthermore, we set $q = 1$ and $\gamma = 1$. Fig. 5 shows the asymptotic distortion for BPSK and QPSK constellations. For the sake of comparison, a lower bound for the asymptotic distortion as proved in Appendix C is also plotted. Moreover, some simulation results obtained by some integer programming are also plotted for BPSK constellation and $N = 100$. For the BPSK case, it is observed that the RS

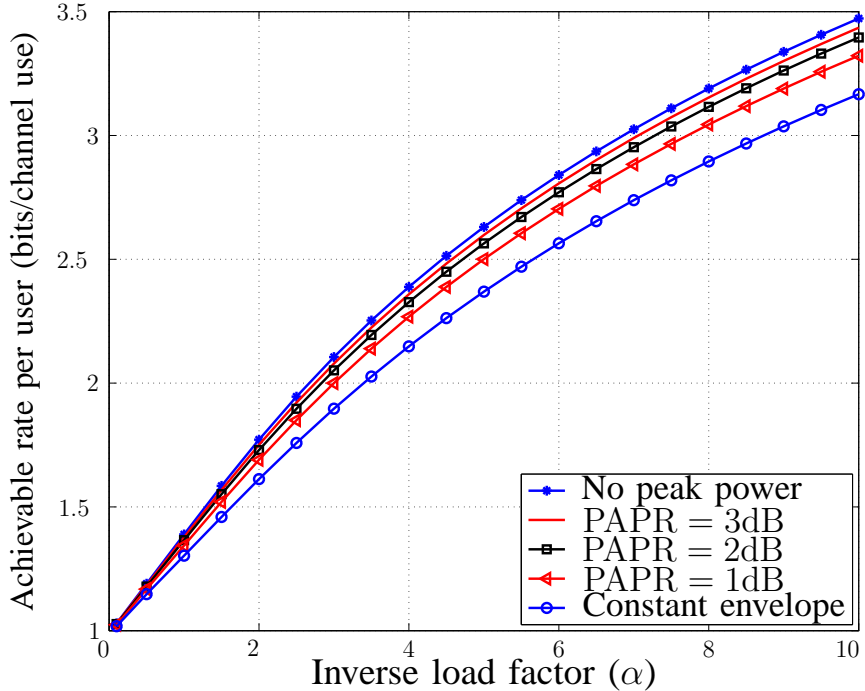


Fig. 3: The achievable rate per user versus the inverse load factor for different PAPR when $q = 1$ and $\sigma_n^2 = 1$. The parameters γ and λ are optimized to fulfill the average power constraint and to maximize the achievable rate.

prediction starts to deviate from the simulation results as α increases. The RS prediction even violates the lower bound for $\alpha \geq 5$. This observation clarifies the failure of the RS assumption in this case. The 1-RSB prediction gives a better prediction than the RS as α grows. However, the 1-RSB prediction also fails to approximate the simulation results and violates the lower bound for large α . This observation brings this conjecture into mind that the precise approximation of the asymptotic distortion is given by the infinite number of replica breaking steps. Similar results are observed for the QPSK constellation.

In order to see the reliability of the solutions in the replica analysis, we plot the entropy versus the inverse load factor in Fig. 6 for BPSK signals. As observed, the 1-RSB solution has much smaller entropy which implies that it is much more reliable than the RS prediction.

Next, we consider M -PSK signals and plot the achievable rate per user terminal versus the inverse load factor α when γ is selected to maximize the achievable rate. Let $q = 1$ and $\sigma_n^2 = 1$.

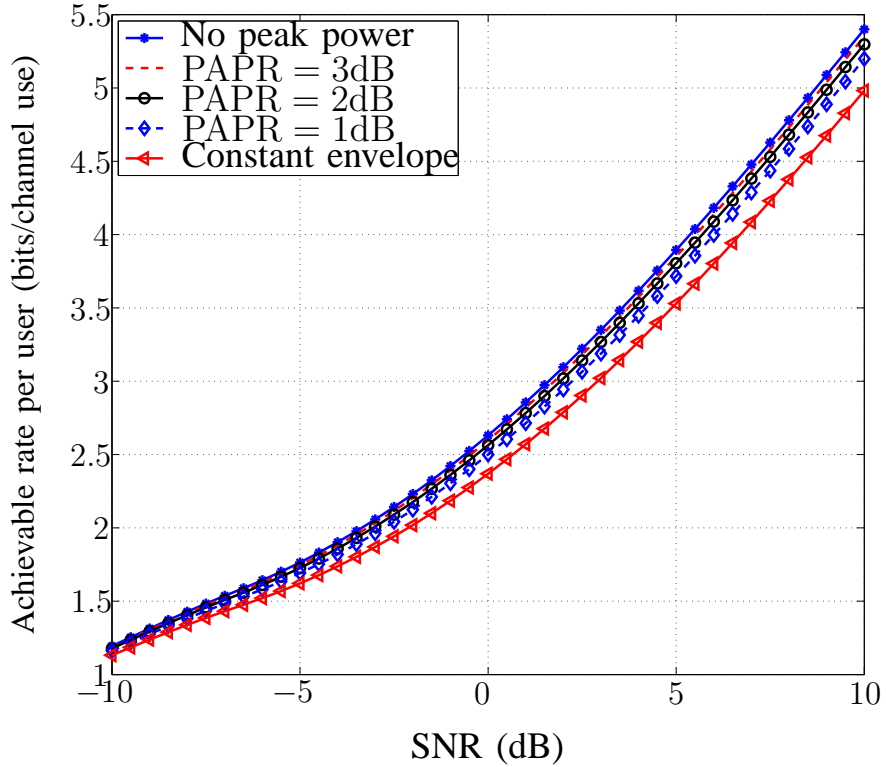


Fig. 4: The achievable rate per user versus the SNR for different PAPR when $q = 1$ and $\alpha = 5$. The parameters γ and λ are optimized to fulfill the average power constraint and to maximize the achievable rate.

The results are given in Fig. 7. The rates for $M \geq 3$ are very close. This means that in MIMO transmitters with LSE precoders, one can use 8-PSK and obtain an acceptable performance instead of using the whole complex unit circle as the support.

VII. CONCLUSIONS AND FUTURE WORKS

In this paper, we analyzed a class of nonlinear precoders called LSE precoders which consider some hardware limitations in massive MIMO systems. The replica method with the RS and the 1-RSB assumptions was used to approximate the achievable rate. The cases of signal with peak power, constant envelope signal on each antenna, finite constellation signal on each antenna were investigated. The results were compared to some simulation results and in the case of PSK signals with a new lower bound. However, there are still some questions which remain open

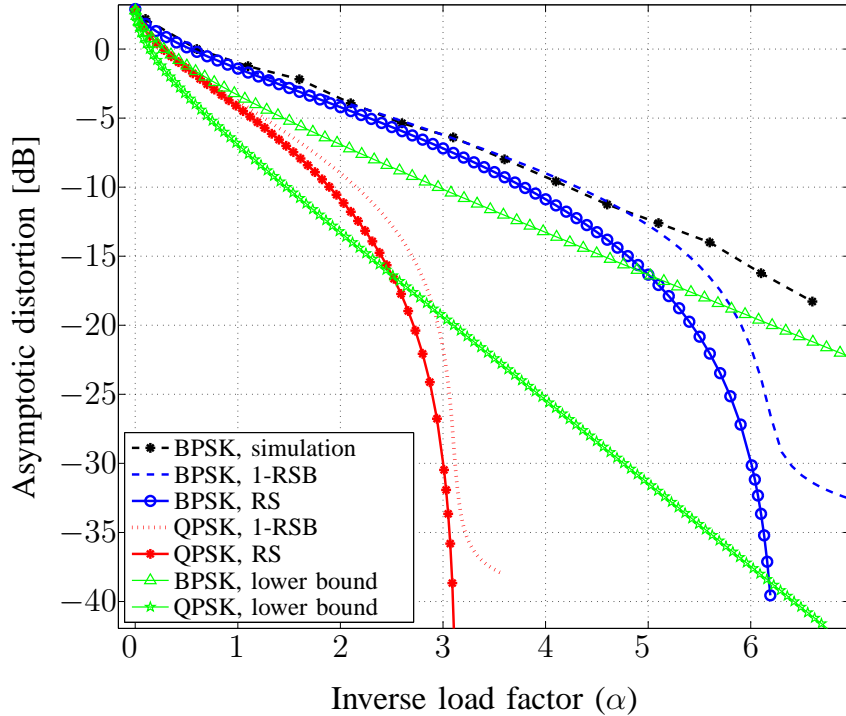


Fig. 5: Asymptotic distortion versus the inverse load factor, i.e., $\alpha = N/K$, for BPSK and QPSK constellations.

in LSE precoders. First, in order to derive the sum rate in a broadcast channel with an LSE precoder, one needs to calculate the joint distribution of the signal of i th user, i.e., u_i and the received signal at the i th user terminal $(\mathbf{Hx})_i$. Note that adding the effect of additive noise at the receive is trivial so is neglected here. Furthermore, the possibility of the decoupling principle in the considered problem is not clear.

As showed in the paper, even 1-RSB solution does not seem to be precise for finite alphabet constellations on each antenna, thus one needs to apply r -step RSB to derive a more precised solution. Another open problem here is to derive the optimum constellation set \mathbb{X} with a given cardinality. This can be done using the RS solution but it seems not to be precise. Finally, practical and feasible algorithm to implement LSE precoders should be investigated.

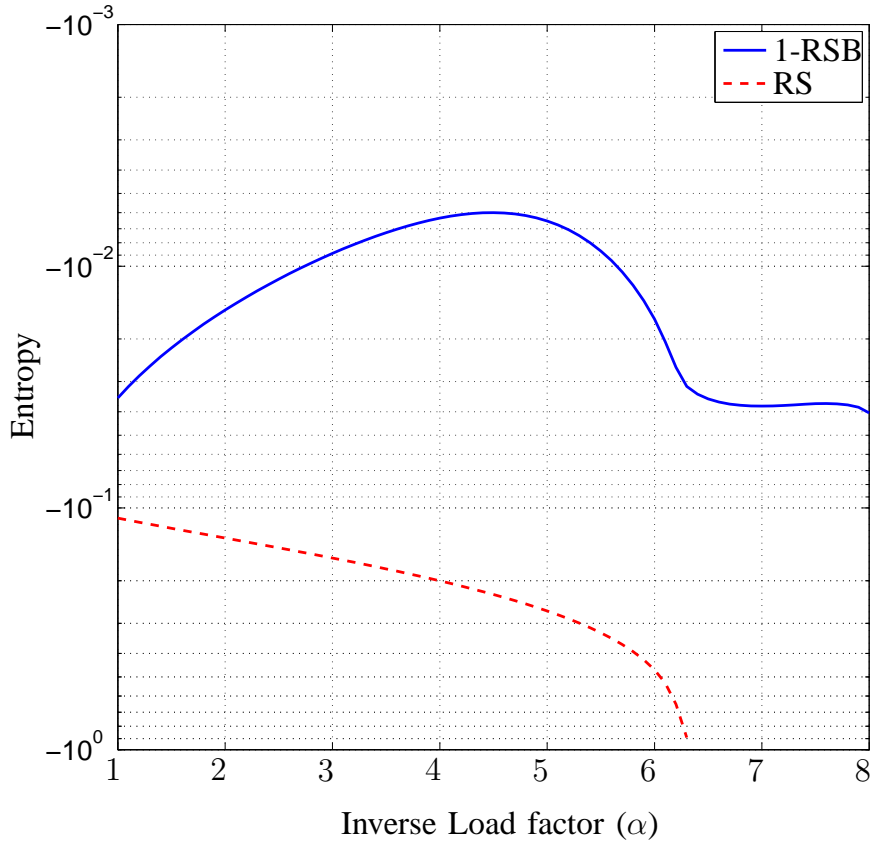


Fig. 6: Entropy of the corresponding thermodynamic system for BPSK signals versus the inverse load factor.

APPENDIX A PROOF OF PROPOSITION 1

Using the RS structure for the matrices \mathbf{Q} and $\tilde{\mathbf{Q}}$, we derive

$$\mathcal{G}(q, \chi) = n\lambda(\beta q + \chi) + (n-1) \int_0^\chi R(-w)dw + \int_0^{\gamma_0} R(-w)dw, \quad (63)$$

where

$$\gamma_0 = \chi - n\chi\beta\gamma\sigma_u^2 + nq\beta - n^2q\beta^2\gamma\sigma_u^2. \quad (64)$$

The integral in (26) is dominated by the maximum argument of the exponential function [15]. The dominant argument is obtained by taking derivative of

$$\mathcal{G}(\mathbf{Q}) + \text{tr}(\tilde{\mathbf{Q}}\mathbf{Q}) \quad (65)$$

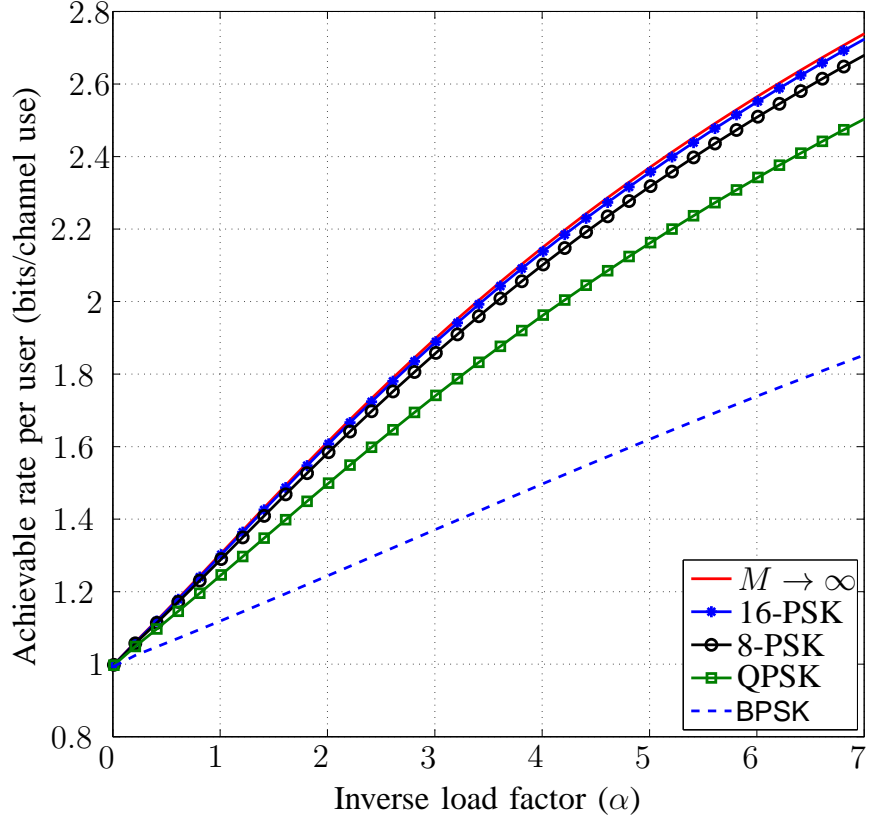


Fig. 7: The achievable rate per user for different PSK schemes versus the inverse load factor based on the RS assumption.

with respect to q and χ which leads to

$$n\lambda + (n - n^2\beta\gamma\sigma_u^2) R_{\mathbf{R}}(-\gamma_0) + n(n-1)\beta f^2 + n(\beta f^2 - e) = 0 \quad (66)$$

$$n\lambda + (n-1)R_{\mathbf{R}}(-\chi) + (1 - n\beta\gamma\sigma_u^2) R_{\mathbf{R}}(-\gamma_0) + n(\beta f^2 - e) = 0. \quad (67)$$

Solving (66)-(67) for f and e results in

$$f = \sqrt{(q - \chi\gamma\sigma_u^2)R'_{\mathbf{R}}(-\chi) + \gamma\sigma_u^2 R(-\chi)} \quad (68)$$

$$e = R_{\mathbf{R}}(-\chi) + \lambda. \quad (69)$$

Using the same argument as in [15, eq. (48)-(58)], we derive the following coupled equations

$$\chi = \frac{1}{f} \int \frac{\sum_{x \in \mathbb{X}} \Re\{z^* x\} e^{2\beta f \Re\{z^* x\} - \beta e|x|^2}}{\sum_{x \in \mathbb{X}} e^{2\beta f \Re\{z^* x\} - \beta e|x|^2}} \quad (70)$$

$$q = \int \frac{\sum_{x \in \mathbb{X}} |x|^2 e^{2\beta f \Re\{z^* x\} - \beta e|x|^2}}{\sum_{x \in \mathbb{X}} e^{2\beta f \Re\{z^* x\} - \beta e|x|^2}} - \frac{\chi}{\beta}. \quad (71)$$

Taking the limit $\beta \rightarrow \infty$, χ and q are obtained as

$$\chi = \frac{\Re \int_{\mathbb{C}} \operatorname{argmin}_{x \in \mathbb{X}} \left| z - \frac{(\mathbf{R}_{\mathbf{R}}(-\chi) + \lambda)x}{\sqrt{(q - \chi\gamma\sigma_u^2)\mathbf{R}'_{\mathbf{R}}(-\chi) + \gamma\sigma_u^2\mathbf{R}(-\chi)}} \right| z^* \frac{e^{-|z|^2}}{\pi} dz}{\sqrt{(q - \chi\gamma\sigma_u^2)\mathbf{R}'_{\mathbf{R}}(-\chi) + \gamma\sigma_u^2\mathbf{R}(-\chi)}} \quad (72)$$

$$q = \int_{\mathbb{C}} \left| \operatorname{argmin}_{x \in \mathbb{X}} \left| z - \left(\frac{\mathbf{R}_{\mathbf{R}}(-\chi) + \lambda)x}{\sqrt{(q - \chi\gamma\sigma_u^2)\mathbf{R}'_{\mathbf{R}}(-\chi) + \gamma\sigma_u^2\mathbf{R}(-\chi)}} \right) \right| \right|^2 \frac{e^{-|z|^2}}{\pi} dz \quad (73)$$

Finally, \check{D} is obtained as

$$\begin{aligned} \check{D} &= \gamma\sigma_u^2 + \lim_{\beta \uparrow \infty} \frac{1}{\beta} \lim_{n \downarrow 0} \frac{\partial}{\partial n} \left[\lambda\alpha n(q\beta + \chi) + \alpha(n-1) \int_0^\chi \mathbf{R}_{\mathbf{R}}(-w) dw + \alpha \int_0^{\gamma_0} \mathbf{R}_{\mathbf{R}}(-w) dw \right. \\ &\quad \left. - \alpha \log(M(e, f)) + \alpha n(n-1)f^2\beta^2q + \alpha n(f^2\beta - e)(\chi + \beta q) \right] \\ &= \gamma\sigma_u^2 + \lambda\alpha q + \alpha \left[q(\mathbf{R}_{\mathbf{R}}(-\chi) - \chi\mathbf{R}'_{\mathbf{R}}(-\chi)) + \sigma_u^2\chi^2\mathbf{R}'_{\mathbf{R}}(-\chi) - 2\chi\sigma_u^2\mathbf{R}_{\mathbf{R}}(-\chi) \right] \\ &= \gamma\sigma_u^2 + \lambda\alpha q + \alpha \frac{\partial}{\partial \chi} \left[(q - \gamma\sigma_u^2\chi)\chi\mathbf{R}_{\mathbf{R}}(-\chi) \right], \end{aligned} \quad (74)$$

and

$$D = \check{D} - \lambda\alpha q = \gamma\sigma_u^2 + \alpha \frac{\partial}{\partial \chi} \left[(q - \gamma\sigma_u^2\chi)\chi\mathbf{R}_{\mathbf{R}}(-\chi) \right]. \quad (75)$$

APPENDIX B

PROOF OF PROPOSITION 2

By applying the the 1-RSB structure, in order to calculate $\mathcal{G}(\mathbf{Q})$, we need to derive the eigenvalues of

$$\begin{aligned} \mathbf{G} &= \Gamma \mathbf{Q} = (-\beta\gamma\sigma_u^2 \mathbf{1}_{n \times n} + \mathbf{I})(q_1 \mathbf{1}_{n \times n} + p_1 \mathbf{I}_{\frac{n\beta}{\mu_1}} \otimes \mathbf{1}_{\frac{\mu_1}{\beta} \times \frac{\mu_1}{\beta}} + \frac{\chi_1}{\beta} \mathbf{I}_{n \times n}) \\ &= (-n\beta\gamma\sigma_u^2 q_1 - \gamma\sigma_u^2 p_1 \mu_1 - \gamma\sigma_u^2 \chi_1 + q_1) \mathbf{1}_{n \times n} + \frac{\chi_1}{\beta} \mathbf{I}_n + p_1 \mathbf{I}_{\frac{n\beta}{\mu_1}} \otimes \mathbf{1}_{\frac{\mu_1}{\beta} \times \frac{\mu_1}{\beta}}. \end{aligned} \quad (76)$$

One can explicitly derive the eigenvalues of \mathbf{G} [16] and obtain

$$\begin{aligned}\mathcal{G}(\mathbf{Q}) &= n\lambda(\chi_1 + \beta(q_1 + p_1)) + \left(n - \frac{n\beta}{\mu_1}\right) \int_0^{\chi_1} \mathbf{R}_{\mathbf{R}}(-w) dw + \left(\frac{n\beta}{\mu_1} - 1\right) \int_0^{\chi_1 + \mu_1 p_1} \mathbf{R}_{\mathbf{R}}(-w) dw \\ &+ \int_0^{\chi_1 + \mu_1 p_1 + \beta n(-n\beta\gamma\sigma_u^2 q_1 - \gamma\sigma_u^2 p_1 \mu_1 - \gamma\sigma_u^2 \chi_1 + q_1)} \mathbf{R}_{\mathbf{R}}(-w) dw.\end{aligned}\quad (77)$$

Furthermore, using the 1-RSB structures for the two matrices \mathbf{Q} and $\tilde{\mathbf{Q}}$, we have

$$\begin{aligned}\text{tr}(\tilde{\mathbf{Q}}\mathbf{Q}) &= n^2\beta^2 f_1^2 q_1 + n\beta f_1^2 p_1 \mu_1 + n\beta f_1^2 \chi_1 + nq_1 \beta g_1^2 \mu_1 + n\beta g_1^2 p_1 \mu_1 \\ &+ n\beta g_1^2 \chi_1 - n\beta e_1 q_1 - n\beta e_1 p_1 - ne_1 \chi_1.\end{aligned}\quad (78)$$

Letting the derivative of

$$\mathcal{G}(\mathbf{Q}) + \text{tr}(\tilde{\mathbf{Q}}\mathbf{Q}) \quad (79)$$

with respect to q_1 , p_1 and χ_1 to zero when $K \rightarrow \infty$ results in

$$\begin{aligned}\lambda + n\beta f_1^2 + \mu_1 g_1^2 - e_1 + (1 - n\beta\gamma\sigma_u^2) \mathbf{R}_{\mathbf{R}}(-\gamma_1) &= 0, \\ \lambda + \mu_1(f_1^2 + g_1^2) - e_1 + \left(1 - \frac{\mu_1}{n\beta}\right) \mathbf{R}_{\mathbf{R}}(-\chi_1 - \mu_1 p_1) + \left(\frac{\mu_1}{n\beta} - \gamma\sigma_u^2 \mu_1\right) \mathbf{R}_{\mathbf{R}}(-\gamma_1) &= 0, \\ \lambda + \beta f_1^2 + \beta g_1^2 - e_1 + \left(1 - \frac{\beta}{\mu_1}\right) \mathbf{R}_{\mathbf{R}}(-\chi_1) + \left(\frac{\beta}{\mu_1} - \frac{1}{n}\right) \mathbf{R}_{\mathbf{R}}(-\chi_1 - \mu_1 p_1) \\ &+ \frac{(1 - \beta n\gamma\sigma_u^2)}{n} \mathbf{R}_{\mathbf{R}}(-\gamma_1) = 0.\end{aligned}\quad (80)$$

where

$$\gamma_1 = \chi_1 + \mu_1 p_1 + \beta n(-n\beta\gamma\sigma_u^2 q_1 - \gamma\sigma_u^2 p_1 \mu_1 - \gamma\sigma_u^2 \chi_1 + q_1). \quad (81)$$

Taking the limit $n \rightarrow 0$, we get

$$\begin{aligned}e_1 &= \mathbf{R}_{\mathbf{R}}(-\chi_1) + \lambda \\ f_1 &= \sqrt{\gamma\sigma_u^2 \mathbf{R}_{\mathbf{R}}(-\chi - \mu_1 p_1) + (q_1 - \gamma\sigma_u^2 \chi_1 - \sigma_u^2 p_1 \mu_1) \mathbf{R}'_{\mathbf{R}}(-\chi - \mu_1 p_1)}, \\ g_1 &= \sqrt{\frac{\mathbf{R}_{\mathbf{R}}(-\chi) - \mathbf{R}_{\mathbf{R}}(-\chi - \mu_1 p_1)}{\mu_1}}.\end{aligned}\quad (82)$$

The Jacobian term $e^{N\mathcal{I}}$ and the coupled equations for f_1, g_1, e_1, μ_1 are obtained using the similar procedure in [16]. The coupled equations in this case become

$$\chi_1 + p_1 \mu_1 = \frac{1}{f_1} \int \int \Re \{ z^* \operatorname{argmin} |f_1 z + g_1 y - e_1 x| \} \tilde{\mathcal{Y}}(y, z) Dz Dy, \quad (83)$$

$$\chi_1 + (q_1 + p_1) \mu_1 = \frac{1}{g_1} \int \int \Re \{ y^* \operatorname{argmin} |f_1 z + g_1 y - e_1 x| \} \tilde{\mathcal{Y}}(y, z) Dz Dy, \quad (84)$$

$$q_1 + p_1 = \int \int |\operatorname{argmin} |f_1 z + g_1 y - e_1 x||^2 \tilde{\mathcal{Y}}(y, z) Dz Dy, \quad (85)$$

$$\begin{aligned} \int_{\chi_1}^{\chi_1 + \mu_1 p_1} R_{\mathbf{R}}(-w) dw &= \int \log \int \mathcal{Y}(y, z) Dy Dz - 2\chi_1 R_{\mathbf{R}}(-\chi_1) \\ &+ (\mu_1 q_1 + 2\chi_1 + 2\mu_1 p_1 - 2p_1 \mu^2 \gamma \sigma_u^2 - 2\chi \mu \gamma \sigma_u^2) R_{\mathbf{R}}(-\chi_1 - \mu_1 p_1) \\ &- 2\mu_1 (q_1 - \gamma \sigma_u^2 \chi - \gamma \sigma_u^2 p_1 \mu_1) (\chi_1 + \mu_1 p_1) R'_{\mathbf{R}}(-\chi_1 - \mu_1 p_1) + \lambda \mu_1 (p_1 + q_1), \end{aligned} \quad (86)$$

where

$$\mathcal{Y}(y, z) \triangleq e^{-\mu_1 \min_{x \in \mathbb{X}} e_1 |x|^2 - 2\Re \{x(f_1 z^* + g_1 y^*)\}}. \quad (87)$$

and

$$\tilde{\mathcal{Y}}(y, z) \triangleq \frac{\mathcal{Y}(y, z)}{\int_{\mathbb{C}} \mathcal{Y}(\tilde{y}, z) D\tilde{y}} \quad (88)$$

Finally, we obtain

$$\begin{aligned} \check{D} &= \gamma \sigma_u^2 + \lim_{\beta \uparrow \infty} \lim_{n \downarrow 0} \frac{\alpha}{\beta} \frac{\partial}{\partial n} n^2 \beta^2 f_1^2 q_1 + n \beta f_1^2 p_1 \mu_1 + n \beta f_1^2 \chi_1 + n q_1 \beta g_1^2 \mu_1 + n \beta g_1^2 p_1 \mu_1 \\ &+ n \beta g_1^2 \chi_1 - n \beta e_1 q_1 - n \beta e_1 p_1 - n e_1 \chi_1 - \log M(\tilde{\mathbf{Q}}) + n \lambda (\chi_1 + \beta (q_1 + p_1)) \\ &+ \left(n - \frac{n \beta}{\mu_1} \right) \int_0^{\chi_1} R_{\mathbf{R}}(-w) dw + \left(\frac{n \beta}{\mu_1} - 1 \right) \int_0^{\chi_1 + \mu_1 p_1} R_{\mathbf{R}}(-w) dw + \int_0^{\gamma_1} R_{\mathbf{R}}(-w) dw, \end{aligned} \quad (89)$$

where we have

$$\log M(\tilde{\mathbf{Q}}) = \log \int \left[\int \left(\sum_{x \in \mathbb{X}} \mathcal{K}(x, y, z) \right)^{\frac{\mu_1}{\beta}} Dy \right]^{\frac{n \beta}{\mu_1}} Dz, \quad (90)$$

and

$$\mathcal{K}(x, y, z) \triangleq e^{2\beta \Re \{x(f_1 z^* + g_1 y^*)\} - \beta e_1 |x|^2}. \quad (91)$$

After some simplification, we obtain

$$\begin{aligned} D &= \gamma \sigma_u^2 - \frac{\alpha \chi_1}{\mu_1} R_{\mathbf{R}}(-\chi_1) + \alpha \left(q_1 + p_1 + \frac{\chi_1}{\mu_1} - 2\gamma \sigma_u^2 (\chi_1 + p_1 \mu_1) \right) R_{\mathbf{R}}(-\chi_1 - \mu_1 p_1) \\ &- \alpha (p_1 \mu_1 + \chi_1) (q - \gamma \sigma_u^2 (\chi_1 + p_1 \mu_1)) R'_{\mathbf{R}}(-\chi_1 - \mu_1 p_1). \end{aligned} \quad (92)$$

APPENDIX C

A LOWER BOUND FOR THE ASYMPTOTIC DISTORTION IN THE CASE OF M-PSK SIGNALS

Let E_K be the event that the minimum distortion is less than ϵ , then

$$P(E_K) = P\left(\min_{\mathbf{x} \in \mathbb{X}^N} \frac{1}{K} \|\mathbf{Hx} - \sqrt{\gamma} \mathbf{u}\|^2 \leq \epsilon\right). \quad (93)$$

From the union bound, we have

$$P(E_K) = P\left(\bigcup_{\mathbf{x} \in \mathbb{X}^N} \frac{1}{K} \|\mathbf{Hx} - \sqrt{\gamma} \mathbf{u}\|^2 \leq \epsilon\right) \leq \sum_{\mathbf{x} \in \mathbb{X}^N} P\left(\frac{1}{K} \|\mathbf{Hx} - \sqrt{\gamma} \mathbf{u}\|^2 \leq \epsilon\right). \quad (94)$$

Let's consider BPSK and QPSK signals. In the large system limit, for iid \mathbf{H} and \mathbf{u} and $\sigma_u^2 = \gamma = 1$, the variable $v = \frac{1}{K} \|\mathbf{Hx} - \mathbf{u}\|^2$ is a scaled chi-square random variable with $2K$ degrees of freedom with the probability density function of

$$f_v(v) = \frac{K^K}{2^K \Gamma(K)} v^{K-1} e^{-\frac{K}{2}v}. \quad (95)$$

Therefore, for M-PSK signals, we have

$$P(E_K) \leq M^{\alpha K} \int_0^{\epsilon} \frac{K^K}{2^K \Gamma(K)} v^{K-1} e^{-\frac{K}{2}v} dv. \quad (96)$$

The function $v^{K-1} e^{-\frac{K}{2}v}$ is an increasing function for small vs . Therefore, a simple upper bound for $P(E_K)$ is

$$P(E_K) \leq M^{\alpha K} \epsilon \frac{K^K}{2^K \Gamma(K)} \epsilon^{K-1} e^{-\frac{K}{2}\epsilon}. \quad (97)$$

For finite α , using the bound [24]

$$\Gamma(K) \geq \sqrt{2\pi} (K-1)^{K-1/2} e^{-K+1}, \quad (98)$$

it can be shown that

$$\lim_{K \uparrow \infty} P(E_K) = 0, \quad (99)$$

if

$$\frac{\epsilon}{2} - \log(\epsilon) > \alpha \log(M) - \log(2) + 1. \quad (100)$$

This gives a lower bound for the asymptotic distortion. For α satisfying (100), the distortion is larger than ϵ in probability in the large system limit. Note that since the probability decays exponentially with K , it can be shown that the statement holds also almost surely using the Borel-Cantelli lemma [25]. Note also that this bound is probably valid only for iid matrices.

APPENDIX D

CHANNEL WITH PATH LOSS EFFECT

The effect of path loss can be considered by using a diagonal matrix \mathbf{D} as

$$\mathbf{H} = \mathbf{D}^{1/2} \mathbf{U}, \quad (101)$$

where k th diagonal element of $\mathbf{D} \triangleq \text{diag}\{d_1, \dots, d_K\}$ is the normalized path loss of the base station to k th user terminal and \mathbf{U} is a $K \times N$ iid matrix whose elements have the variance equal to $1/N$. Let's assume that the users are located in a annular region around the base station uniformly. The maximum and minimum distances to the base station are shown by r_{\max} and r_{\min} , respectively, and the ratio of these distances is defined as $\kappa \triangleq \frac{r_{\max}}{r_{\min}}$.

Let's assume that the path loss factors d_1, \dots, d_K are normalized such that the path loss for the users located at the distance of r_{\min} is 1. Then, Considering the path loss exponent of ν , one can derive the distribution of the path loss factor d_k for $k = 1, \dots, K$ as

$$f_d(d) = \frac{2}{\nu(\kappa^2 - 1)d^{\frac{2}{\nu}+1}}. \quad (102)$$

Since the results in this paper only depend on the distribution of the eigenvalues of the matrix $\mathbf{R} = \mathbf{H}^\dagger \mathbf{H}$, we investigate the effect of this path loss model to the R-transform of \mathbf{R} . Using the following lemma, we derive the Stieltjes transform of the distribution of the eigenvalues of the matrix $\mathbf{R} = \mathbf{U}^\dagger \mathbf{D} \mathbf{U}$.

LEMMA 1 *The Stieltjes transform of \mathbf{R} satisfies [26]*

$$\frac{1}{G_{\mathbf{R}}(s)} + s = \alpha \int \frac{zf_d(z)dz}{\alpha + zG_{\mathbf{R}}(s)}. \quad (103)$$

Then, the R-transform $R_{\mathbf{R}}(w)$ is obtained numerically using the relation between Stieltjes transform and R-transform as shown in (20). We do not present the numerical results for the case with path loss effect, since the results in this case follow the same behavior as in the iid matrix case.

E GENERALIZATION TO FREQUENCY-SELECTIVE FADING CHANNELS

Let L be the number of sub-carriers and also assume that the channel is frequency-flat at each frequency sub-band. For simplicity, assume that each sub-band includes one sub-carrier. Furthermore, let \mathbf{H}_j be the channel matrix at j th frequency sub-band with iid entries. The data input vector at the i th sub-carrier is denoted by \mathbf{u}_i .

We consider a MIMO-OFDM approach. The base station first precodes the data vectors for the sub-carriers and then uses one Inverse Fast Fourier Transform (IFFT) block per antenna. The LSE precoder in this case determines L column vectors $\mathbf{v}_1, \dots, \mathbf{v}_L$ to be given to the IFFT blocks as inputs. \mathbf{v}_i is the input vector for the IFFT block of the i th antenna. Let \mathbf{W} be the IFFT matrix and $\mathbf{v}_t \triangleq \text{Vec}([\mathbf{v}_1, \dots, \mathbf{v}_L]^T)$. The LSE precoder rule is

$$\mathbf{v}_t = \underset{\mathbf{W}_t \mathbf{x}_t \in \mathbb{X}^{NL}}{\operatorname{argmin}} \|\mathbf{H}_t \mathbf{x}_t - \sqrt{\gamma} \mathbf{u}_t\|^2 + \lambda \|\mathbf{x}_t\|^2, \quad (104)$$

where \mathbf{H}_t is a $KL \times NL$ matrix whose k th part of its $(i-1)L+k$ columns is the i th column of the \mathbf{H}_k and the remained entries are zero, $\mathbf{u}_t \triangleq [\mathbf{u}_1^T, \dots, \mathbf{u}_L^T]^T$ and \mathbf{W}_t is an $LN \times LN$ block-diagonal matrix whose $L \times L$ diagonal blocks are equal to \mathbf{W} .

One can reformulate (104) as

$$\mathbf{v}_t = \underset{\mathbf{z}_t \in \mathbb{X}^{NL}}{\operatorname{argmin}} \|\mathbf{H}_t \mathbf{W}_t^\dagger \mathbf{z}_t - \sqrt{\gamma} \mathbf{u}_t\|^2 + \lambda \|\mathbf{z}_t\|^2, \quad (105)$$

using the fact that $\mathbf{W}_t \mathbf{W}_t^\dagger = \mathbf{I}$. One can consider an equivalent frequency-flat fading channel with the channel matrix equal to $\mathbf{H}_t \mathbf{W}_t^\dagger$. For the case that \mathbf{H}_i s are iid matrices, Fig. 8 compares the empirical cumulative distribution of the eigenvalues of $\mathbf{R}_t = \mathbf{H}_t^\dagger \mathbf{H}_t$ and $\mathbf{R}_j = \mathbf{H}_j^\dagger \mathbf{H}_j$ numerically for $L = 64$ and $K = N = 128$. It is observed that the both cases have the same distribution for iid binary and Gaussian cases. Since the result derived by the replica method depends only on the eigenvalue distribution of \mathbf{R}_t , this shows that the LSE precoder in this case has the same performance as in the case of frequency-flat fading channel.

REFERENCES

- [1] M. A. Sedaghat, A. Bereyhi, and R. Müller, “A new class of nonlinear precoders for hardware efficient massive MIMO systems,” submitted to *IEEE International Conference on Communications (ICC), Paris*, 2017.
- [2] F. Rusek, D. Persson, B. K. Lau, E. G. Larsson, T. L. Marzetta, O. Edfors, and F. Tufvesson, “Scaling up MIMO: Opportunities and challenges with very large arrays,” *Signal Processing Magazine, IEEE*, vol. 30, no. 1, pp. 40–60, 2013.
- [3] C. B. Peel, B. M. Hochwald, and A. L. Swindlehurst, “A vector-perturbation technique for near-capacity multiantenna multiuser communication-Part I: Channel inversion and regularization,” *IEEE Transactions on Communications*, vol. 53, no. 1, pp. 195–202, Jan. 2005.
- [4] R. F. Fischer, C. Windpassinger, A. Lampe, and J. B. Huber, “Space-time transmission using tomlinson-harashima precoding,” *ITG FACHBERICHT*, pp. 139–148, 2002.
- [5] B. M. Hochwald, C. Peel, and A. Swindlehurst, “A vector-perturbation technique for near-capacity multiantenna multiuser communication-Part II: Perturbation,” *IEEE Transactions on Communications*, vol. 53, no. 3, pp. 537–544, Mar. 2005.

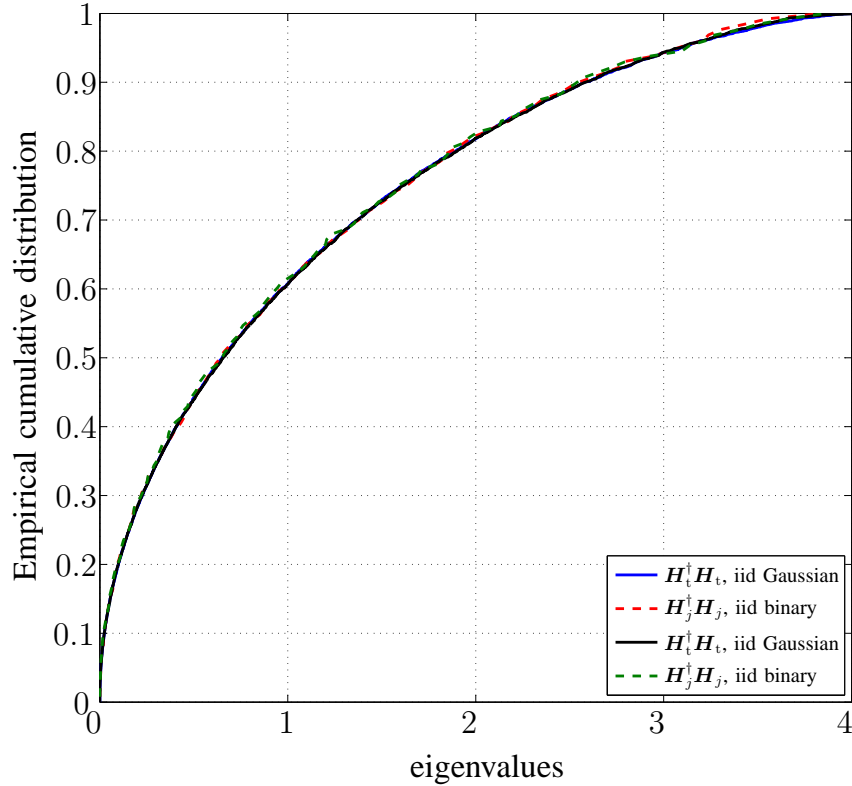


Fig. 8: Empirical cumulative distribution of two matrices $\mathbf{H}_t^\dagger \mathbf{H}_t$ and $\mathbf{H}_j^\dagger \mathbf{H}_j$ for $L = 64$ and $N = K = 128$.

- [6] W. Zeng, C. Xiao, M. Wang, and J. Lu, “Linear precoding for finite-alphabet inputs over MIMO fading channels with statistical csi,” *Signal Processing, IEEE Transactions on*, vol. 60, no. 6, pp. 3134–3148, 2012.
- [7] A. Wiesel, Y. C. Eldar, and S. Shamai, “Zero-forcing precoding and generalized inverses,” *Signal Processing, IEEE Transactions on*, vol. 56, no. 9, pp. 4409–4418, 2008.
- [8] M. A. Sedaghat, V. I. Barousis, C. Papadias *et al.*, “Load modulated arrays: a low-complexity antenna,” *IEEE Communications Magazine*, vol. 54, no. 3, pp. 46–52, 2016.
- [9] M. Sedaghat, R. Müller, G. Fischer, and A. Ali, “Discrete load-modulated single-RF MIMO transmitters,” in *Workshop on Smart Antennas (WSA)*, 2015, pp. 1–7.
- [10] S. K. Mohammed and E. G. Larsson, “Constant-envelope multi-user precoding for frequency-selective massive MIMO systems,” *Wireless Communications Letters, IEEE*, vol. 2, no. 5, pp. 547–550, 2013.
- [11] ———, “Per-antenna constant envelope precoding for large multi-user MIMO systems,” *Communications, IEEE Transactions on*, vol. 61, no. 3, pp. 1059–1071, 2013.
- [12] M. Sedaghat, R. Müller, and G. Fischer, “Broadcast precoding for massive MIMO subject to an instantaneous total power constraint,” in *IEEE Global Communications Conference (Globecom)*, 2014, pp. 1–5.
- [13] M. A. Sedaghat, R. R. Müller, and G. Fischer, “A novel single-RF transmitter for massive MIMO,” in *Smart Antennas*

(WSA), 2014 18th International ITG Workshop on. VDE, 2014.

- [14] D. Guo and S. Verdú, “Randomly spread CDMA: Asymptotics via statistical physics,” *IEEE Transactions on Information Theory*, vol. 51, no. 6, pp. 1983–2010, Jun. 2005.
- [15] R. R. Müller, D. Guo, and A. L. Moustakas, “Vector precoding for wireless MIMO systems: A replica analysis,” *IEEE Journal on Selected Areas in Communications*, vol. 26, no. 3, pp. 530–540, Apr. 2008.
- [16] B. M. Zaïdel, R. R. Müller, A. L. Moustakas, and R. De Miguel, “Vector precoding for gaussian MIMO broadcast channels: Impact of replica symmetry breaking,” *Information Theory, IEEE Transactions on*, vol. 58, no. 3, pp. 1413–1440, 2012.
- [17] S. S. Varadhan, “Asymptotic probabilities and differential equations,” *Communications on Pure and Applied Mathematics*, vol. 19, no. 3, pp. 261–286, 1966.
- [18] M. Talagrand, “Mean field models for spin glasses: a first course,” *Lectures on probability theory and statistics (Saint-Flour, 2000)*, vol. 1816, pp. 181–285, 2000.
- [19] A. Guionnet and M. Maïda, “A Fourier view on the R-transform and related asymptotics of spherical integrals,” *Journal of Functional Analysis*, vol. 222, pp. 435–490, 2005.
- [20] T. Tanaka, “A statistical mechanics approach to large-system analysis of CDMA multiuser detectors,” *IEEE Transactions on Information Theory*, vol. 48, no. 11, pp. 2888–2910, Nov. 2002.
- [21] A. Montanari and D. Tse, “Analysis of belief propagation for non-linear problems: The example of cdma (or: How to prove tanaka’s formula),” in *Information Theory Workshop, 2006. ITW’06 Punta del Este. IEEE*. IEEE, 2006, pp. 160–164.
- [22] G. Reeves and H. D. Pfister, “The replica-symmetric prediction for compressed sensing with gaussian matrices is exact,” in *Information Theory (ISIT), 2016 IEEE International Symposium on*. IEEE, 2016, pp. 665–669.
- [23] A. M. Tulino and S. Verdú, “Random matrix theory and wireless communications,” *Foundations and Trends in Communications and Information Theory*, vol. 1, no. 1, Jun. 2004.
- [24] H. Robbins, “A remark on stirling’s formula,” *The American Mathematical Monthly*, vol. 62, no. 1, pp. 26–29, 1955.
- [25] P. Brémaud, *An introduction to probabilistic modeling*. Springer Science & Business Media, 2012.
- [26] R. Couillet and M. Debbah, *Random matrix methods for wireless communications*. Cambridge University Press, 2011.